ANTIMICROBIAL AGENTS AND CHEMOTHERAPY, July 2007, p. 2329–2336 Vol. 51, No. 7
0066-4804/07/$08.00+0 doi:10.1128/AAC.00185-07

Isoniazid Bactericidal Activity and Resistance Emergence: Integrating Pharmacodynamics and Pharmacogenomics To Predict Efficacy in Different Ethnic Populations▽

Tawanda Gumbo,[1,2]* Arnold Louie,[2] Weiguo Liu,[2] David Brown,[2] Paul G. Ambrose,[2,3] Sujata M. Bhavnani,[2,3] and George L. Drusano[2,3]

Divison of Infectious Diseases, UT Southwestern Medical Center, Dallas, Texas 75390,[1] and Emerging Infections and Host Defense Section[2] and Institute for Clinical Pharmacodynamics, Ordway Research Institute,[3] Albany, New York 12208

Received 7 February 2007/Returned for modification 20 March 2007/Accepted 9 April 2007

Isoniazid, administered as part of combination antituberculosis therapy, is responsible for most of the early bactericidal activity (EBA) of the regimen. However, the emergence of *Mycobacterium tuberculosis* resistance to isoniazid is a major problem. We examined the relationship between isoniazid exposure and *M. tuberculosis* microbial kill, as well as the emergence of resistance, in our in vitro pharmacodynamic model of tuberculosis. Since single-nucleotide polymorphisms of the *N*-acetyltransferase-2 gene lead to two different clearances of isoniazid from serum in patients, we simulated the isoniazid concentration-time profiles encountered in both slow and fast acetylators. Both microbial kill and the emergence of resistance during monotherapy were associated with the ratio of the area under the isoniazid concentration-time curve from 0 to 24 h ($AUC_{0–24}$) to the isoniazid MIC. The time in mutant selection window hypothesis was rejected. Next, we utilized the in vitro relationship between the isoniazid $AUC_{0–24}$/MIC ratio and microbial kill, the distributions of isoniazid clearance in populations with different percentages of slow and fast acetylators, and the distribution of isoniazid MICs for isonazid-susceptible *M. tuberculosis* clinical isolates in Monte Carlo simulations to calculate the EBA expected for ~10,000 patients treated with 300 mg of isoniazid. For those patient populations in which the proportion of fast acetylators and the isoniazid MICs were high, the average EBA of the standard dose was ~0.3 $\log_{10}$ CFU/ml/day and was thus suboptimal. Our approach, which utilizes preclinical pharmacodynamics and the genetically determined multimodal distributions of serum clearances, is a preclinical tool that may be able to predict the EBAs of various doses of new antituberculosis drugs.

In the 21st century, tuberculosis is still responsible for 3% of all human deaths (45). First-line antituberculosis therapy consists of isoniazid, pyrazinamide, and rifampin. It is thought that isoniazid kills the largest population of *Mycobacterium tuberculosis*, which represents bacilli in log-phase growth, after which pyrazinamide kills the slower-growing population of bacilli in acidic milieus and rifampin kills nonreplicating bacilli (4, 23, 29, 33). Isoniazid microbial kill ceases after 2 to 3 days of therapy. As a result, isoniazid's microbial kill in patients is measured using an index termed early bactericidal activity (EBA), which is the average rate of sputum bacillary decline during the first 2 days of therapy (10, 23). It is also believed that the cessation of kill is due to depletion of bacilli in the log phase of growth. However, we recently demonstrated that this early cessation of kill by isoniazid is due to the emergence of an isoniazid-resistant population (20). The pharmacokinetic-pharmacodynamic (PK-PD) relationship between isoniazid exposure and the emergence of resistance is, as yet, unknown.

The pharmacokinetics and pharmacogenomics of isoniazid in humans have been well characterized. The concentration of isoniazid in human serum declines due to metabolism by arylamine *N*-acetyltransferase-2 (NAT2). Single-nucleotide polymorphisms (SNPs) of the NAT2 gene lead to two human phenotypes: fast acetylators, in whom the half-life of isoniazid in serum is 0.9 to 1.8 h, and slow acetylators, in whom the half-life is 2.2 to 4.4 h (14, 32). Therefore, the area under the isoniazid concentration-time curve from 0 to 24 h ($AUC_{0–24}$) and the percentage of the dosing interval during which the isoniazid concentration is above the MIC (T_{MIC}) will differ between fast and slow acetylators who receive the same dose of isoniazid. Different ethnic populations have different distributions of fast and slow acetylators (7, 25, 28, 34), and after they receive the same isoniazid dose (e.g., 300 mg a day), different percentages of patients for each population will achieve a particular isoniazid $AUC_{0–24}$. Therefore, the overall efficacy of the currently recommended dose of isoniazid may differ between different ethnic groups. Thus, the efficacy of the standard dose in different patient populations needs to be reexamined.

In the current study, we identified the PK-PD index ($AUC_{0–24}$/MIC ratio, T_{MIC}, or the ratio of the peak concentration of isoniazid in serum to the MIC [C_{max}/MIC]) that best explained isoniazid's microbial kill. We utilized this relationship in Monte-Carlo simulations to determine the bactericidal activities expected from administering the recommended isoniazid dose to different ethnic populations, given the different distributions of NAT2 gene SNPs and the distribution of isonazid MICs for

* Corresponding author. Mailing address: Division of Infectious Diseases, UT Southwestern Medical Center, 5323 Harry Hines Blvd., Dallas, TX 75390-9113. Phone: (214) 648-9914. Fax: (214) 648-2741. E-mail: Tawanda.Gumbo@UTSouthwestern.edu.

▽ Published ahead of print on 16 April 2007.

M. tuberculosis clinical isolates. We also examined the relationship between the PK-PD index and the emergence of isoniazid resistance. Since it has been suggested that the percentage of the dosing interval during which an antibiotic concentration is within the mutant selection window (T_{MSW}) is closely associated with the emergence of resistance (12, 16, 47), we also examined whether the T_{MSW} is indeed linked to isoniazid resistance. The mutant selection window is the concentration range above the MIC of an antibiotic to the pathogen but below the concentration that prevents selection of the first step of mutation that confers drug resistance. It should be noted that resistance emergence during monotherapy was studied. It is standard clinical practice to administer combination therapy so that the drugs in the combination can reduce the emergence of resistance to one another (4, 33). Therefore, our results must be interpreted in this context.

MATERIALS AND METHODS

Bacterial isolate. *M. tuberculosis* H37Ra (American Type Culture Collection, Manassas, VA) cultures were stored at −80°C in Middlebrook 7H9 broth (Becton Dickinson, Sparks, MD). For each study, aliquots were thawed and incubated under 5% CO_2 at 37°C in Middlebrook 7H9 broth for 4 days.

Drugs. Isoniazid was purchased from Sigma-Aldrich (St. Louis, MO). The drug was dissolved in sterile water to the desired concentrations.

MIC, mutation frequency, and MPC. Isoniazid MIC testing was performed using methods recommended by the Clinical and Laboratory Standards Institute (formerly NCCLS) (5). The frequency of mutation in response to isoniazid was determined by plating a total of 2 ml of a 10^8-CFU/ml *M. tuberculosis* suspension onto Middlebrook 7H10 agar containing either 0.2 or 1.0 mg of isoniazid/liter; these concentrations define low-level and high-level clinical resistance, respectively (5). The mutation prevention concentration (MPC) was determined using methods described by Drlica and colleagues (12, 36). All cultures were incubated at 37°C under 5% CO_2 and were read after 3 weeks.

Isoniazid dose range studies in an in vitro pharmacodynamic model of tuberculosis. Full details of our experimental in vitro pharmacodynamic model of tuberculosis have been described previously (18–20). This experimental system allows *M. tuberculosis* in log-phase growth to be exposed to isoniazid concentration-time profiles similar to those observed in the serum of humans, so that clinical regimens can be simulated. *M. tuberculosis* in Middlebrook 7H9 broth enriched with 10% oleic acid-albumin-dextrose-catalase and 0.025% Tween 80 was incubated in flasks under shaking conditions under 5% CO_2 at 37°C. On the 4th day of growth, *M. tuberculosis* cultures were used to determine the frequency of mutation in response to 0.2 and 1.0 mg of isoniazid/liter (5). The cultures were then diluted in prewarmed Middlebrook 7H9 broth to a final density of 10^6 CFU/ml, and 15 ml of the bacterial suspension was inoculated into each of the eight experimental systems. Starting 24 h later, isoniazid treatment was administered daily for 7 days to simulate serum isoniazid concentration-time profiles in humans treated with 0, 25, 100, or 300 mg a day (for both slow and fast acetylators) or with 600 mg a day (for fast acetylators). These doses were chosen based on prior studies (20). The doses achieve isoniazid AUC_{0-24} exposures of 0, 1.7, 6.8, and 20 mg · h/liter for slow acetylator phenotypes and 0.6, 2.4, 7.1, and 14.2 mg · h/liter for fast acetylators, based on the serum isoniazid clearances published by Peloquin et al. (32). The in vitro pharmacodynamic systems were sampled to confirm that the intended isoniazid concentrations had been achieved as well as to determine the size of the total microbial population and the *M. tuberculosis* populations resistant to 0.2 and 1.0 mg of isoniazid/liter.

Measurement of isoniazid concentrations. Isoniazid concentrations in media collected from the experimental systems were measured by high-pressure liquid chromatography. The assay characteristics were the same as those described for a previous study (20).

Studies to characterize *katG* mutations and efflux pumps in isoniazid resistance. Three isoniazid-resistant *M. tuberculosis* isolates per day were selected from each treatment regimen, and mutations in the *katG* gene were determined using methods described by Parsons et al. (31). To examine the role of efflux pumps in isoniazid resistance (6, 42), we used our in vitro experimental system in a separate experiment to simulate treatment of *M. tuberculosis* infection with an isoniazid dose of 0 mg daily, 300 mg daily, or 900 mg as a single dose at day 0. Slow acetylator concentration-time profiles were mimicked. The isoniazid doses of 300 mg once daily and a single dose of 900 mg have the same AUC of 60 mg · h/liter at the end of 3 days, which is the end of isoniazid EBA in our in vitro model (20). On days 0, 2, 3, and 5 of therapy, 0.8-ml cultures were sampled from the experimental systems and were divided into two equal portions. Reserpine was added to one portion to a final concentration of 1.0 mg/liter, and then the sample was incubated at 37°C for 15 min. Ethidium bromide, which fluoresces with a concentration-dependent intensity when in contact with bacterial DNA, was added to both portions to a final concentration of 10 mg/liter in a volume of 0.5 ml. The cultures were incubated at 37°C for 30 min. Counts and fluorescence intensity were examined in a Cytomics FC500 flow cytometer (Coulter Cytometry Systems, Miami, FL) at an excitation wavelength of 530 nm and an emission wavelength of 630 nm. Counts were set to 10,000 events.

Pharmacokinetic and mathematical modeling. Population pharmacokinetic analysis was performed using the nonparametric adaptive grid algorithm. A one-compartment open model with first-order input and elimination was utilized. The mean pharmacokinetic parameters that we calculated from these studies were then used, in conjunction with the MIC and MPC, to calculate the isoniazid half-life, C_{max}/MIC, AUC_{0-24}/MIC, T_{MIC}, and T_{MSW}.

The relationship between isoniazid exposure and microbial kill was analyzed using the inhibitory sigmoid E_{max} model with a variable slope, defined by the equation $E = E_{con} - [(E_{max} \times EC^H)/(EC^H + EC_{50}{}^H)]$, where E is the observed *M. tuberculosis* $\log_{10}$ CFU/ml, E_{con} is the bacillary $\log_{10}$ CFU/ml in the control arm, E_{max} is the maximal antimicrobial effect on bacillary density ($\log_{10}$ CFU/ml) with isoniazid therapy, EC is the isoniazid drug exposure, EC_{50} is the drug exposure that achieves 50% of maximal effect, and H is Hill's constant. The E_{max} at the end of effective microbial kill was divided by the number of days of effective microbial kill to give an estimate of in vitro EBA (CFU/ml/day).

Our next step was performance of Monte Carlo simulations, to integrate the isoniazid PK-PD relationship, isoniazid population pharmacokinetics, and isoniazid's microbial kill. We utilized the population pharmacokinetics of isoniazid described by Peloquin et al. (32) as input into the PRIOR subroutine of the ADAPT II program (8). In the Monte Carlo simulation, a population of 9,999 virtual patients given 300 mg of isoniazid was examined to generate a distribution of serum drug clearances. The 9,999 iterates were chosen in order to stabilize the variance in the tails of the distribution. Due to different distributions of *nat2* SNPs, different ethnic populations of the world have different proportions of fast and slow acetylators. We incorporated a bimodal distribution of clearances to reflect slow-acetylator proportions (expressed as percentages) of patients in Shanghai, China (12%) (28) and in the United States (67%) (32), populations at either end of the spectrum. The simulation also took into account the different isoniazid MICs between 0.008 and 0.256 mg/liter to calculate PK-PD exposure values, since different geographic regions have different susceptibility patterns (27, 46). By using the inhibitory sigmoid E_{max} relationship between isoniazid exposure and microbial kill derived from the in vitro experiments, the population of patients was examined to determine the microbial kill expected from administering 300 mg of isoniazid a day orally to the patients.

Computer software. Population pharmacokinetic analysis was performed using the nonparametric adaptive grid software program of Leary and colleagues (26). Monte Carlo simulations were carried out using the ADAPT II software of D'Argenio and Schumitzky (8). Sigmoid E_{max} analyses were performed using GraphPad Prism, version 4 (GraphPad Software, San Diego, CA), which runs on Windows. All the programs ran on a personal computer, with the ADAPT II program requiring a Fortran compiler.

RESULTS

MIC, mutation frequency, and MPC. The isoniazid MIC for the *M. tuberculosis* isolate was 0.0156 mg/liter. The prevalence of mutants resistant to 0.2 mg of isoniazid/liter was 1 in 1.8×10^5 to 1 in 7.9×10^5 CFU, and that of mutants resistant to 1.0 mg of isoniazid/liter was 1 in 9.8×10^5 to 1 in 18.2×10^5 CFU. The MPC was 50 mg/liter; thus, the upper and lower boundaries of the mutant selection window were 0.0156 and 50 mg/liter, respectively.

Isoniazid microbial kill. Isoniazid declined with a half-life of either 4.16 h or 1.84 h in our experimental system, consistent with slow and fast acetylation, respectively. Isoniazid-mediated decline in total microbial density ceased after day 3 (data not shown). Examination of the relationship between PK-PD indi-

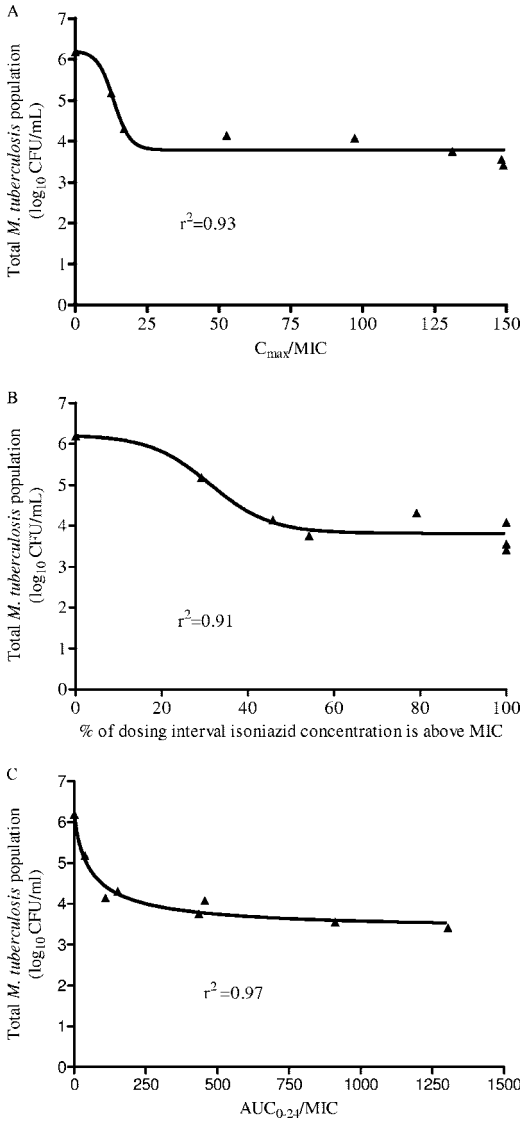

FIG. 1. Relationship between pharmacodynamic indices and microbial kill on day 3. Data are shown for C_{max}/MIC (A), T_{MIC} (B), and AUC_{0-24}/MIC (C).

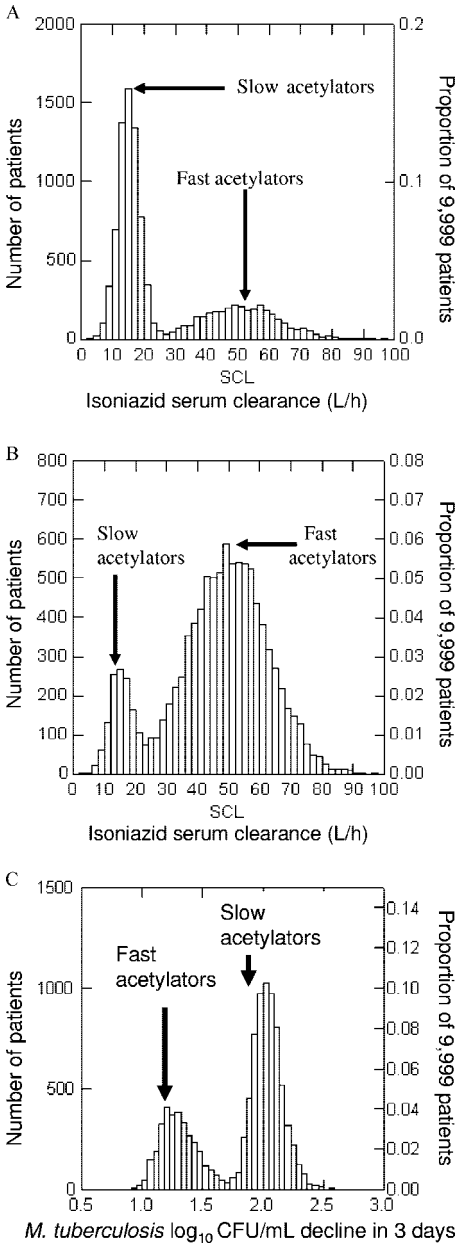

FIG. 2. Distribution of isoniazid clearance from serum and the resultant bactericidal activity derived from Monte Carlo simulations. (A and B) Serum clearance for a U.S. population (A) and the Chinese population of Shanghai (B). (C) Bactericidal activity achieved in a group of U.S. patients.

ces and microbial kill for day 3 revealed that the PK-PD index most explanatory of isoniazid microbial kill was the AUC_{0-24}/MIC ratio (Fig. 1A to C), described by the following equation: $\log_{10}$ CFU/ml = 6.20 − {[2.89 × $(AUC_{0-24}/MIC)^{0.9}$]/[$(AUC_{0-24}/MIC)^{0.9}$ + $61.55^{0.9}$]} ($P < 0.01$), where 2.89 $\log_{10}$ CFU/ml is the E_{max} and 61.55 is the AUC_{0-24}/MIC ratio mediating 50% of the E_{max}. For days 1 and 2, the r^2 values for AUC_{0-24}/MIC were 0.94 and 0.97, compared to 0.78 and 0.03 for C_{max}/MIC and 0.86 and 0.70 for T_{MIC}, respectively ($P < 0.01$).

The day 3 relationship between AUC_{0-24}/MIC and microbial kill was used in Monte Carlo simulations to predict the total microbial kill and EBA expected with administration of 300 mg of isoniazid to patients. Figure 2A and B demonstrate the distribution of serum isoniazid clearances in 9,999 simulated American and Chinese patients, respectively, given the proportions of slow and fast acetylators in these two respective populations. These serum clearances directly determine the isoniazid AUC_{0-24} for each patient, and each of these AUC_{0-24} values will effect a specific degree of microbial kill as specified by the inhibitory sigmoid E_{max} equation given above. An example is the bactericidal effect in the American patients infected with *M. tuberculosis* isolates for which the isoniazid MIC is 0.12 mg/liter (Fig. 2C). A summation at each MIC for each of the two populations of patients is shown in Fig. 3. There is a decrease in EBA as the isoniazid MIC increases, even within the MIC range considered to reflect isoniazid susceptibility. This is particularly significant in populations with high percentages of fast acetylators, in which the average EBA falls to a

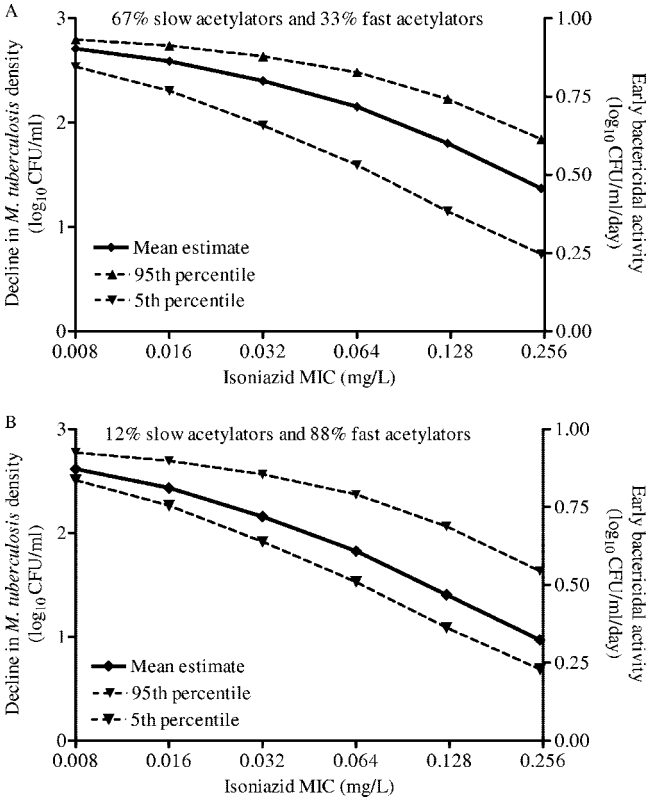

FIG. 3. EBA in patients, derived from Monte Carlo simulations. Results are shown for a U.S. population (A) and the Chinese population of Shanghai (B). EBA is shown on the right *y* axis.

suboptimal ~0.3 $\log_{10}$ CFU/ml/day at the upper end of the MIC range.

Emergence of isoniazid resistance. The PK-PD indices associated with both low-level and high-level isoniazid resistance were examined for each of the 7 days of therapy. Since no isoniazid concentration in our study exceeded the MPC, the T_{MSW} was equal to the T_{MIC}. For each simulated dose, slow acetylation was associated with a longer T_{MSW} than fast acetylation. However, the sizes of the resistant populations were similar for slow and fast acetylators (Fig. 4A to C). When a sigmoid E_{max} model was fit to the T_{MSW} and the size of each of the two resistant subpopulations, the model was such a poor fit to the data that the computer program failed to reach any meaningful solution to the sigmoid E_{max} model equation for 12 of 14 regressions. The first exception was for day 6 data, which revealed an r^2 of 0.51. However, the relationship revealed that a T_{MSW} of <5% mediated a 50% increase in resistance, a finding inconsistent with the T_{MSW} hypothesis. The second exception was for day 5 high-level resistance data, which, however, revealed an r^2 of only 0.39. Taken together, the T_{MSW} hypothesis was rejected.

The relationship between time, the density of the resistant subpopulation, and the concentration-dependent PK-PD indices (C_{max}/MIC or AUC_{0-24}/MIC) was described by a U-shaped curve starting on day 1 of therapy, suggesting an initial diminution of the resistant population with therapy (Fig. 5A and B). However, as the duration of therapy increased, there was a

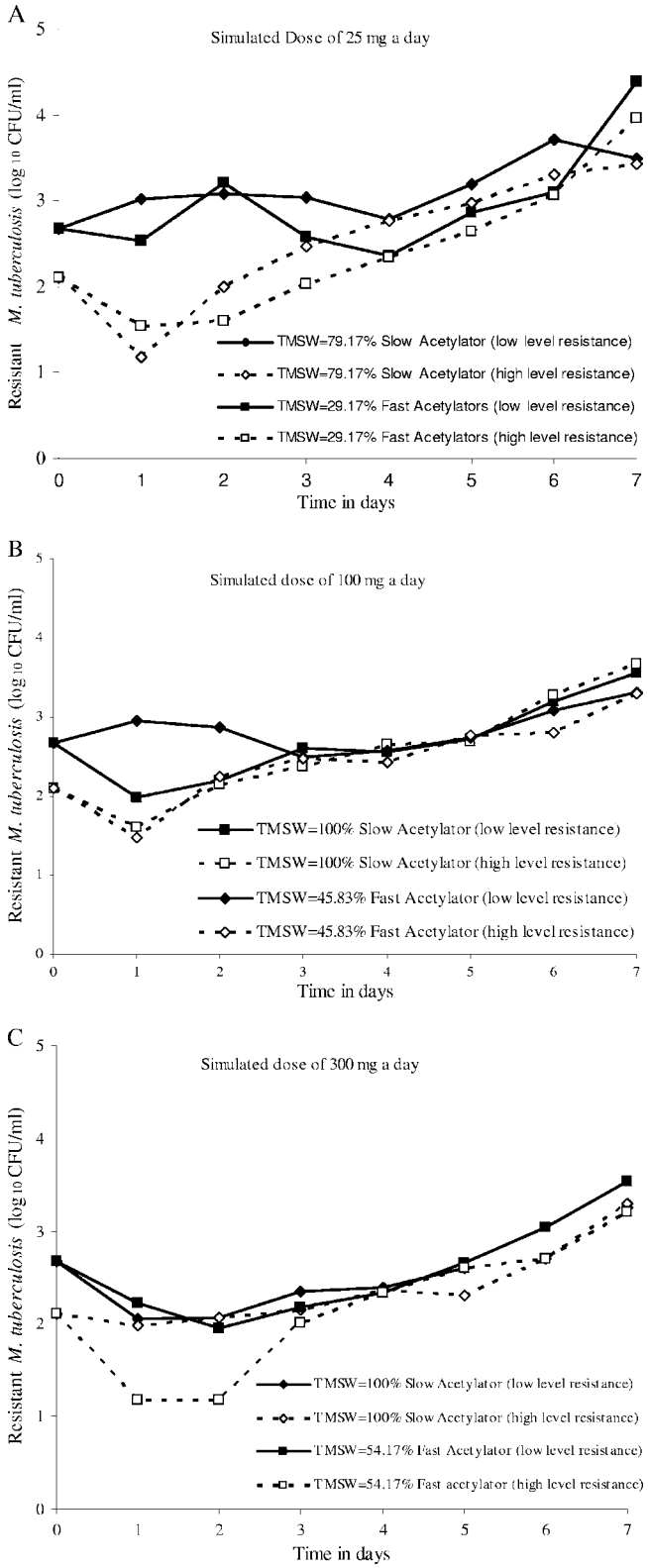

FIG. 4. T_{MSW} does not predict the emergence of resistance. For each isoniazid dose examined, slow acetylation status, which is associated with a greater T_{MSW}, had the same effect on resistance as fast acetylation status.

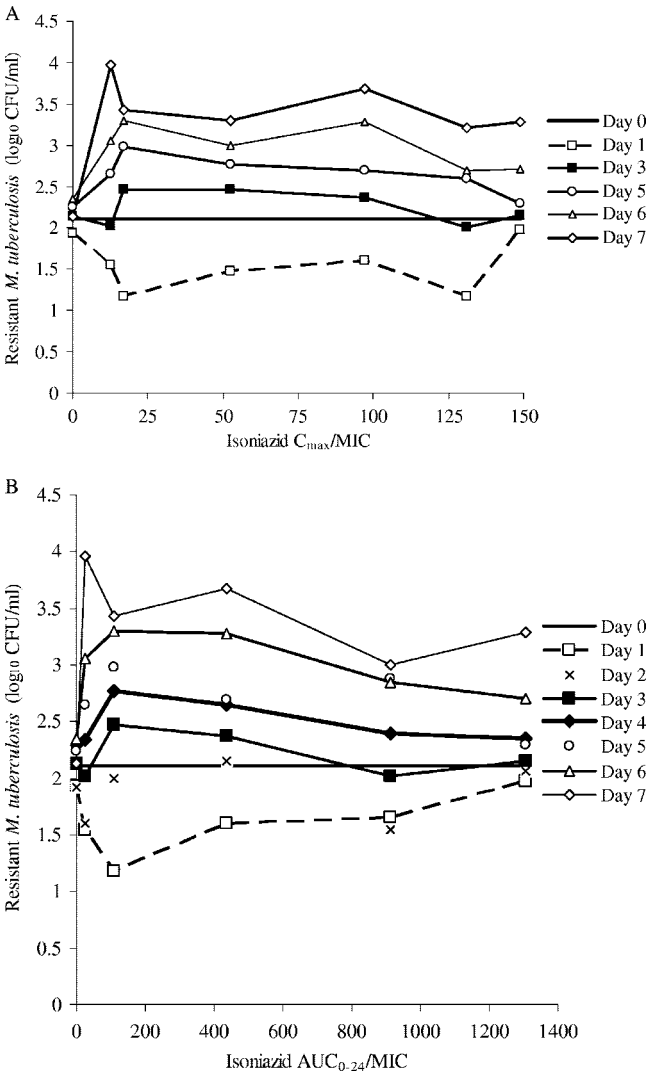

FIG. 5. Relationship between concentration-dependent indices (C_{max}/MIC, AUC/MIC) and the size of the resistant population. Shown are day-to-day changes in resistant population levels with respect to increases in the C_{max}/MIC ratio (A) and the AUC_{0-24}/MIC ratio (B). Each line represents the change in the resistant population with a change in the PK-PD index value on a particular day of therapy. Only data for the population with high-level resistance are shown; the pattern for low-level resistance curves is similar. Lines for some of the days, such as day 2, were not drawn for purposes of clarity.

transition to an inverted U-shaped curve on day 3, demonstrating amplification of the resistant subpopulation. As the duration of therapy increased beyond day 3, higher drug exposures were needed to reduce resistance, and by day 7 no isoniazid exposures tested could suppress resistance.

Resistant isolates from these experiments revealed single point mutations in *katG* codon 300 of resistant isolates from the bacterial suspension used to inoculate the hollow fiber systems, both in the untreated controls and in all treatment groups, indicating that this mutation was present prior to the initiation of isoniazid therapy. In the isoniazid treatment groups, mutations in *katG* codons 315, 321, and 322 arose on the third day of therapy. In separate experiments, isoniazid-treated cultures from day 3 onward revealed an 18 to 24% increase in ethidium bromide fluorescence for bacilli that had been preincubated with reserpine compared to those that had not been pretreated. Control cultures had no changes in fluorescence. These data are consistent with reserpine-inhibitable efflux pumps.

DISCUSSION

Tuberculosis is currently treated with combination therapy. However, studying and optimizing monotherapy regimens will allow for optimal efficacy of combination antituberculosis therapy regimens. Moreover, during the first 2 to 5 days of antituberculosis therapy in patients, the EBA of combination therapy is derived mainly from isoniazid's microbial kill of log-phase *M. tuberculosis* (23, 24). In these early phases of therapy, the isoniazid PK-PD index associated with microbial kill in our in vitro model was the AUC_{0-24}/MIC ratio. This is similar to the results from a study by Jayaram et al. with an aerosol mouse model of tuberculosis (22). This is also consistent with the fact that for patients with tuberculosis, the isoniazid AUC strongly correlates with EBA (11). It is also interesting that even when isoniazid was given in combination with rifapentine, in U.S. Public Health Service study 22, patients with low isoniazid AUC_{0-12} values were more likely to fail therapy than patients with higher isoniazid AUC_{0-12} values (44). This suggests that PK-PD lessons from our in vitro models may also apply to long-term outcomes for patients.

In our in vitro study, the relationship between the isoniazid AUC/MIC ratio and microbial kill was described by an E_{max} of 2.89 $\log_{10}$ CFU/ml (in vitro maximal EBA, 0.9 $\log_{10}$ CFU/ml/day), an EC_{50} (AUC_{0-24}/MIC) of 61.6, and an H of 0.9. The AUC_{0-24} that corresponds with the EC_{50} is 1.0 mg · h/liter. In the murine studies of Jayaram et al., the E_{max} was 1.3 $\log_{10}$ CFU/lung, H was 1.0, and the EC_{50} (AUC_{0-24}/MIC) was 63.0 (22). The values for these parameters are remarkably similar to ours. The differences in the E_{max} between the mice and our in vitro model simply reflect the fact that the two studies used two different end points in terms of bacillary burden: the total CFU in a whole mouse lung versus the CFU/ml in liquid medium. It is also unclear if the EC_{50} in the murine studies refers to total exposure or free drug. Even so, after any possible correction for protein binding, the EC_{50} would still be within the same range as the EC_{50} we derived. Similarly, our analysis of an isoniazid dose-versus-EBA study of South African patients (9) using the sigmoid E_{max} model yielded the following model estimates: E_{max}, 0.6 ± 0.2 $\log_{10}$ CFU/ml/day; H, 1.2; EC_{50}, 1.3 mg/kg of body weight/day ($r^2 = 0.99$; $P < 0.001$). Since this population consisted predominantly of fast acetylators, the EC_{50} corresponds to a mean AUC_{0-24} of 1.3 (9, 11, 32). These results are also remarkably similar to those we derived in vitro. The E_{max} that we calculated for these patients is likely an underestimate, because we utilized reported mean EBA values. This is consistent with the fact that in the inhibitory sigmoid E_{max} relationship, the E_{max} (efficacy), the EC_{50} (potency), and H (the strength of microbial kill in response to changes in the AUC_{0-24}/MIC ratio) are determined mostly by the interaction of the particular drug and the particular microbial species and are thus expected to be similar in many biological systems.

We utilized the relationship between the AUC_{0-24}/MIC

ratio and microbial kill from our in vitro pharmacodynamic model to predict the EBAs for different patient groups treated with an isoniazid dose of 300 mg a day. Our approach takes into account the published population pharmacokinetics of isoniazid, including the bimodal distribution of serum clearance and the percentages of patients who are fast versus slow acetylators in different ethnic populations. As an example, we predict that for patients in Chennai, India, where 62% of patients are slow acetylators (34) and the isoniazid MIC is ≤0.032 mg/liter for 70% of isolates (41), the average EBA (95% confidence interval [95% CI]) will be 0.90 (0.40 to 0.93) $\log_{10}$ CFU/ml/day. In Cape Town, South Africa, where 56 to 67% of patients are fast acetylators and the isoniazid MIC is thought to be 0.1 mg/liter (1, 9, 11), the EBA (95% CI) is predicted to be ~ 0.60 (0.38 to 0.74) $\log_{10}$ CFU/ml/day. On the other hand, in Hong Kong, where 23% of the patients are slow acetylators and the isoniazid MIC is 0.1 to 0.2 mg/liter, we predict an EBA (95% CI) of 0.40 (0.23 to 0.69) $\log_{10}$ CFU/ml/day (38, 39). These predictions are highly concordant with the results of a multicenter clinical trial that observed the lowest mean EBA (95% CI), 0.37 (0.16 to 0.58) $\log_{10}$ CFU/ml/day, in Hong Kong; an intermediate EBA, 0.65 (0.43 to 0.87) $\log_{10}$ CFU/ml/day, in Cape Town; and the highest EBA, 0.94 (0.45 to 1.43) $\log_{10}$ CFU/ml/day, in Chennai (37). One would expect that in areas such as Japan, where the isoniazid MIC for 80% of isolates is ≥0.125 mg/liter (46) and the proportion of fast acetylator phenotypes is ~90% (25), the standard isoniazid dose of 300 mg a day would have a mean EBA of ~0.3 $\log_{10}$ CFU/ml/day, which is suboptimal.

Our modeling approach gives us a tool to predict the bactericidal activities of new antituberculosis compounds. Thus, even prior to clinical EBA studies, reasonable predictions of the bactericidal effects of different doses of the drug would be made. Clinical studies could then be carried out with doses that have the highest EBA, if such doses can be tolerated by patients. Another important contribution of the current study is the incorporation of multimodal elimination of an antituberculosis compound into Monte Carlo simulations to predict microbial effect. Such an application will enable modeling that could predict the clinical effects of the new antituberculosis compounds that have multimodal elimination. An example that comes to mind is the phenothiazine thioridazine, which has recently stimulated interest because of its antituberculosis activity (17, 30). Thioridazine is metabolized by CYP2D6 enzymes, and SNPs of the *CYP2D6* gene lead to four human phenotypes: poor, intermediate, extensive, and ultrarapid metabolizers (2, 3). These CYP2D6 SNPs show wide differences in distribution between different ethnic groups (2, 3). Once thioridazine PK-PD studies have been successfully performed, our approach, in which the population frequencies of the drug's multimodal elimination are taken into consideration, may help predict the thioridazine EBAs for different ethnic populations.

While it is important to identify regimens that optimize microbial kill, identifying doses that reduce the emergence of resistance is also vitally important (13). We demonstrated that the emergence of isoniazid resistance did not correlate closely with T_{MSW}. Instead, resistance was concentration dependent. It is interesting that in U.S. Public Health Service study 23, in which isoniazid was combined with rifabutin, patients who developed rifamycin resistance and relapse had lower isoniazid AUC_{0-12} values than those without failure (43). This result suggests that in fact the isoniazid AUC may also be linked to the prevention of resistance to companion drugs in combination therapy. However, these clinical trial results are probably more reflective of events during the continuation phase of therapy than of the initial phases of therapy.

The relationship between isoniazid concentration and isoniazid resistance was complex and at some time points was reminiscent of the inverted-U curve that we have described for the effects of fluoroquinolone on *Klebsiella pneumoniae* and *Staphylococcus aureus* (40). In the inverted-U relationship, the fluroquinolone-resistant subpopulations initially increased and then decreased with increasing exposure, until a threshold AUC_{0-24}/MIC ratio that prevented resistance amplification was attained (40). In the current study, we examined the relationship between a nonquinolone compound and a bacterium that has a long doubling time, which allowed us to examine more closely the relationship between exposure, resistance, and time. With 1 day of treatment, the locus of the point describing the relationship between exposure and the size of the resistant subpopulation is below that on day 0 and is described by a shape that roughly approximates an upright U-shaped curve. This indicates that a portion of the preexistent resistant subpopulation was killed in a concentration-dependent manner during the first few days. However the U shape inverted on day 3, coincident with the end of microbial kill and the emergence of an isoniazid-resistant population exhibiting efflux pumps and the type of *katG* mutations commonly encountered in isoniazid-resistant clinical isolates (21, 35). From day 3 onward, the curves were shaped like inverted U's, indicating resistance amplification. As the duration of isoniazid therapy increased, a time was reached when no exposures tested were able to suppress resistance.

Our study has several limitations. First, the experiments were carried out using an in vitro system; thus, they may not completely reflect events in vivo. In addition, we utilized an avirulent *M. tuberculosis* strain for our studies, not the virulent strain. However, the in vitro pharmacodynamics of other antibiotic compounds have been demonstrated to be similar whether avirulent or virulent *M. tuberculosis* strains are used (15). In addition, the concordance of our results with those for mice and for patients suggests that our conclusions are correct. Second, our in vitro study was not designed to examine the sterilizing activity of isoniazid. Such studies will be performed in the future. Third, we did not study the strategy of adding a second drug to reduce the emergence of resistance. This, too, will be examined in the future. Nevertheless, it is interesting that in clinical studies of isoniazid and rifamycin combinations, relapse as well as the emergence of rifamycin resistance was associated with the isoniazid AUC (43, 44). This suggests that the concentration-dependent effect of isoniazid on the emergence of resistance to companion drugs is likely to be important, which is why each of the drugs in the combination needs to be optimized. Finally, while reserpine-inhibitable efflux pumps have been reported in vitro, they have so far not been reported in the clinical arena (6, 42).

In summary, isoniazid microbial kill and the emergence of resistance were concentration dependent. The relationship between concentration and the isoniazid-resistant population was

described by a system of U-shaped curves, which inverted as the duration of therapy increased. The relationship between concentration and microbial kill was exploited in Monte Carlo simulations to predict the EBAs of recommended doses of isoniazid in different ethnic groups, and for some groups the effect was suboptimal.

ACKNOWLEDGMENT

We acknowledge the financial support of the Charitable Leadership Foundation, Clifton Park, NY.

REFERENCES

1. **Adams, C. H., C. J. Werely, T. C. Victor, E. G. Hoal, G. Rossouw, and P. D. van Helden.** 2003. Allele frequencies for glutathione *S*-transferase and *N*-acetyltransferase 2 differ in African population groups and may be associated with oesophageal cancer or tuberculosis incidence. Clin. Chem. Lab. Med. **41:**600–605.
2. **Berecz, R., A. de la Rubia, P. Dorado, P. Fernandez-Salguero, M. L. Dahl, and A. Llerena.** 2003. Thioridazine steady-state plasma concentrations are influenced by tobacco smoking and CYP2D6, but not by the CYP2C9 genotype. Eur. J. Clin. Pharmacol. **59:**45–50.
3. **Bernard, S., K. A. Neville, A. T. Nguyen, and D. A. Flockhart.** 2006. Interethnic differences in genetic polymorphisms of CYP2D6 in the U.S. population: clinical implications. Oncologist **11:**126–135.
4. **Blumberg, H. M., W. J. Burman, R. E. Chaisson, C. L. Daley, S. C. Etkind, L. N. Friedman, P. Fujiwara, M. Grzemska, P. C. Hopewell, M. D. Iseman, R. M. Jasmer, V. Koppaka, R. I. Menzies, R. J. O'Brien, R. R. Reves, L. B. Reichman, P. M. Simone, J. R. Starke, and A. A. Vernon.** 2003. American Thoracic Society/Centers for Disease Control and Prevention/Infectious Diseases Society of America: treatment of tuberculosis. Am. J. Respir. Crit. Care Med. **167:**603–662.
5. **Clinical and Laboratory Standards Institute.** 2003. Susceptibility testing of mycobacteria, nocardiae, and other aerobic actinomycetes; approved standard. Clinical and Laboratory Standards Institute, Wayne, PA.
6. **Colangeli, R., D. Helb, S. Sridharan, J. Sun, M. Varma-Basil, M. H. Hazbon, R. Harbacheuski, N. J. Megjugorac, W. R. Jacobs, Jr., A. Holzenburg, J. C. Sacchettini, and D. Alland.** 2005. The *Mycobacterium tuberculosis iniA* gene is essential for activity of an efflux pump that confers drug tolerance to both isoniazid and ethambutol. Mol. Microbiol. **55:**1829–1840.
7. **Dandara, C., C. M. Masimirembwa, A. Magimba, S. Kaaya, J. Sayi, D. K. Sommers, J. R. Snyman, and J. A. Hasler.** 2003. Arylamine *N*-acetyltransferase (NAT2) genotypes in Africans: the identification of a new allele with nucleotide changes 481C>T and 590G>A. Pharmacogenetics **13:**55–58.
8. **D'Argenio, D. Z., and A. Schumitzky.** 1997. ADAPT II. A program for simulation, identification, and optimal experimental design. User manual. Biomedical Simulations Resource, University of Southern California, Los Angeles.
9. **Donald, P. R., F. A. Sirgel, F. J. Botha, H. I. Seifart, D. P. Parkin, M. L. Vandenplas, B. W. Van de Wal, J. S. Maritz, and D. A. Mitchison.** 1997. The early bactericidal activity of isoniazid related to its dose size in pulmonary tuberculosis. Am. J. Respir. Crit. Care Med. **156:**895–900.
10. **Donald, P. R., F. A. Sirgel, A. Venter, D. P. Parkin, H. I. Seifart, B. W. Van de Wal, J. S. Maritz, and P. B. Fourie.** 2003. Early bactericidal activity of antituberculosis agents. Expert Rev. Anti-Infect. Ther. **1:**141–155.
11. **Donald, P. R., F. A. Sirgel, A. Venter, D. P. Parkin, H. I. Seifart, B. W. Van de Wal, C. Werely, P. D. van Helden, and J. S. Maritz.** 2004. The influence of human *N*-acetyltransferase genotype on the early bactericidal activity of isoniazid. Clin. Infect. Dis. **39:**1425–1430.
12. **Dong, Y., X. Zhao, B. N. Kreiswirth, and K. Drlica.** 2000. Mutant prevention concentration as a measure of antibiotic potency: studies with clinical isolates of *Mycobacterium tuberculosis*. Antimicrob. Agents Chemother. **44:**2581–2584.
13. **Drusano, G. L., A. Louie, M. Deziel, and T. Gumbo.** 2006. The crisis of resistance: identifying drug exposures to suppress amplification of resistant mutant subpopulations. Clin. Infect. Dis. **42:**525–532.
14. **Evans, D. A., K. A. Manley, and V. A. McKusick.** 1960. Genetic control of isoniazid metabolism in man. Br. Med. J. **2:**485–491.
15. **Fietta, A., M. Morosini, and A. Cascina.** 2001. Effects of continuous or pulsed exposure to rifabutin and sparfloxacin on the intracellular growth of *Staphylococcus aureus* and *Mycobacterium tuberculosis*. J. Chemother. **13:**167–175.
16. **Firsov, A. A., S. N. Vostrov, I. Y. Lubenko, K. Drlica, Y. A. Portnoy, and S. H. Zinner.** 2003. In vitro pharmacodynamic evaluation of the mutant selection window hypothesis using four fluoroquinolones against *Staphylococcus aureus*. Antimicrob. Agents Chemother. **47:**1604–1613.
17. **Global Alliance for TB Drug Development.** 2006. RFP 2006 01. Preclinical evaluation of new drug combinations against tuberculosis. Global Alliance for TB Drug Development, New York, NY.
18. **Gumbo, T., A. Louie, M. R. Deziel, and G. L. Drusano.** 2005. Pharmacodynamic evidence that ciprofloxacin failure against tuberculosis is not due to poor microbial kill but to rapid emergence of resistance. Antimicrob. Agents Chemother. **49:**3178–3181.
19. **Gumbo, T., A. Louie, M. R. Deziel, L. M. Parsons, M. Salfinger, and G. L. Drusano.** 2004. Selection of a moxifloxacin dose that suppresses drug resistance in *Mycobacterium tuberculosis*, by use of an in vitro pharmacodynamic infection model and mathematical modeling. J. Infect. Dis. **190:**1642–1651.
20. **Gumbo, T., A. Louie, W. Liu, P. G. Ambrose, S. M. Bhavnani, D. Brown, and G. L. Drusano.** 2007. Isoniazid's bactericidal activity ceases because of the emergence of resistance, not depletion of *Mycobacterium tuberculosis* in the log phase of growth. J. Infect. Dis. **195:**194–201.
21. **Haas, W. H., K. Schilke, J. Brand, B. Amthor, K. Weyer, P. B. Fourie, G. Bretzel, V. Sticht-Groh, and H. J. Bremer.** 1997. Molecular analysis of *katG* gene mutations in strains of *Mycobacterium tuberculosis* complex from Africa. Antimicrob. Agents Chemother. **41:**1601–1603.
22. **Jayaram, R., R. K. Shandil, S. Gaonkar, P. Kaur, B. L. Suresh, B. N. Mahesh, R. Jayashree, V. Nandi, S. Bharath, E. Kantharaj, and V. Balasubramanian.** 2004. Isoniazid pharmacokinetics-pharmacodynamics in an aerosol infection model of tuberculosis. Antimicrob. Agents Chemother. **48:**2951–2957.
23. **Jindani, A., V. R. Aber, E. A. Edwards, and D. A. Mitchison.** 1980. The early bactericidal activity of drugs in patients with pulmonary tuberculosis. Am. Rev. Respir. Dis. **121:**939–949.
24. **Jindani, A., C. J. Dore, and D. A. Mitchison.** 2003. Bactericidal and sterilizing activities of antituberculosis drugs during the first 14 days. Am. J. Respir. Crit. Care Med. **167:**1348–1354.
25. **Katoh, T., R. Boissy, N. Nagata, K. Kitagawa, Y. Kuroda, H. Itoh, T. Kawamoto, and D. A. Bell.** 2000. Inherited polymorphism in the *N*-acetyltransferase 1 (NAT1) and 2 (NAT2) genes and susceptibility to gastric and colorectal adenocarcinoma. Int. J. Cancer **85:**46–49.
26. **Leary, R., R. Jellife, A. Schumitzky, and M. Van Guilder.** 2001. An adaptive grid non-parametric approach to pharmacokinetic and dynamic (PK/PD) models. IEEE Computer Society, Bethesda, MD.
27. **Lee, C. N., and L. B. Heifets.** 1987. Determination of minimal inhibitory concentrations of antituberculosis drugs by radiometric and conventional methods. Am. Rev. Respir. Dis. **136:**349–352.
28. **Ma, Q. W., G. F. Lin, J. G. Chen, C. Q. Xiang, W. C. Guo, K. Golka, and J. H. Shen.** 2004. Polymorphism of *N*-acetyltransferase 2 (NAT2) gene polymorphism in Shanghai population: occupational and non-occupational bladder cancer patient groups. Biomed. Environ. Sci. **17:**291–298.
29. **Mitchison, D. A.** 1979. Basic mechanisms of chemotherapy. Chest **76:**771–781.
30. **Ordway, D., M. Viveiros, C. Leandro, R. Bettencourt, J. Almeida, M. Martins, J. E. Kristiansen, J. Molnar, and L. Amaral.** 2003. Clinical concentrations of thioridazine kill intracellular multidrug-resistant *Mycobacterium tuberculosis*. Antimicrob. Agents Chemother. **47:**917–922.
31. **Parsons, L. M., M. Salfinger, A. Clobridge, J. Dormandy, L. Mirabello, V. L. Polletta, A. Sanic, O. Sinyavskiy, S. C. Larsen, J. Driscoll, G. Zickas, and H. W. Taber.** 2005. Phenotypic and molecular characterization of *Mycobacterium tuberculosis* isolates resistant to both isoniazid and ethambutol. Antimicrob. Agents Chemother. **49:**2218–2225.
32. **Peloquin, C. A., G. S. Jaresko, C. L. Yong, A. C. Keung, A. E. Bulpitt, and R. W. Jelliffe.** 1997. Population pharmacokinetic modeling of isoniazid, rifampin, and pyrazinamide. Antimicrob. Agents Chemother. **41:**2670–2679.
33. **Rieder, H. L.** 2002. Interventions for tuberculosis control and elimination. International Union against Tuberculosis and Lung Diseases, Paris, France.
34. **Sarma, G. R., S. Kailasam, M. Datta, G. K. Loganathan, F. Rahman, and A. S. Narayana.** 1990. Classification of children as slow or rapid acetylators based on concentrations of isoniazid in saliva following oral administration of body-weight and surface-area-related dosages of the drug. Indian Pediatr. **27:**134–142.
35. **Silva, M. S., S. G. Senna, M. O. Ribeiro, A. R. Valim, M. A. Telles, A. Kritski, G. P. Morlock, R. C. Cooksey, A. Zaha, and M. L. Rossetti.** 2003. Mutations in *katG*, *inhA*, and *ahpC* genes of Brazilian isoniazid-resistant isolates of *Mycobacterium tuberculosis*. J. Clin. Microbiol. **41:**4471–4474.
36. **Sindelar, G., X. Zhao, A. Liew, Y. Dong, T. Lu, J. Zhou, J. Domagala, and K. Drlica.** 2000. Mutant prevention concentration as a measure of fluoroquinolone potency against mycobacteria. Antimicrob. Agents Chemother. **44:**3337–3343.
37. **Sirgel, F. A., P. R. Donald, J. Odhiambo, W. Githui, K. C. Umapathy, C. N. Paramasivan, C. M. Tam, K. M. Kam, C. W. Lam, K. M. Sole, and D. A. Mitchison.** 2000. A multicentre study of the early bactericidal activity of anti-tuberculosis drugs. J. Antimicrob. Chemother. **45:**859–870.
38. **Suo, J., C. E. Chang, T. P. Lin, and L. B. Heifets.** 1988. Minimal inhibitory concentrations of isoniazid, rifampin, ethambutol, and streptomycin against *Mycobacterium tuberculosis* strains isolated before treatment of patients in Taiwan. Am. Rev. Respir. Dis. **138:**999–1001.
39. **Tam, C. M., S. L. Chan, K. M. Kam, R. L. Goodall, and D. A. Mitchison.** 2002. Rifapentine and isoniazid in the continuation phase of a 6-month regimen. Final report at 5 years: prognostic value of various measures. Int. J. Tuberc. Lung Dis. **6:**3–10.

40. **Tam, V. H., A. Louie, M. R. Deziel, W. Liu, and G. L. Drusano.** 2007. The relationship between quinolone exposures and resistance amplification is characterized by an inverted U: a new paradigm for optimizing pharmacodynamics to counterselect resistance. Antimicrob. Agents Chemother. **51:** 744–747.
41. **Varma, M., S. Kumar, A. Kumar, and M. Bose.** 2002. Comparison of Etest and agar proportion method of testing drug susceptibility of *M. tuberculosis*. Indian J. Tuberc. **490:**217–220.
42. **Viveiros, M., I. Portugal, R. Bettencourt, T. C. Victor, A. M. Jordaan, C. Leandro, D. Ordway, and L. Amaral.** 2002. Isoniazid-induced transient high-level resistance in *Mycobacterium tuberculosis*. Antimicrob. Agents Chemother. **46:**2804–2810.
43. **Weiner, M., D. Benator, W. Burman, C. A. Peloquin, A. Khan, A. Vernon, B. Jones, C. Silva-Trigo, Z. Zhao, and T. Hodge.** 2005. Association between acquired rifamycin resistance and the pharmacokinetics of rifabutin and isoniazid among patients with HIV and tuberculosis. Clin. Infect. Dis. **40:** 1481–1491.
44. **Weiner, M., W. Burman, A. Vernon, D. Benator, C. A. Peloquin, A. Khan, S. Weis, B. King, N. Shah, and T. Hodge.** 2003. Low isoniazid concentrations and outcome of tuberculosis treatment with once-weekly isoniazid and rifapentine. Am. J. Respir. Crit. Care Med. **167:**1341–1347.
45. **World Health Organization.** 2004. Global burden of disease estimates. DTH6 2002Rev. http://www.who.int/healthinfo/bodestimates/en/.
46. **Yamane, N., I. Nakasone, H. Saitoh, M. Kaneda, M. Shimojima, K. Yamashita, K. Toyoda, and Y. Okazawa.** 1998. Evaluation of a newly developed broth microdilution test method to determine minimum inhibitory concentrations (MICs) of antimicrobial agents for mycobacteria. Rinsho Byori **46:**719–727.
47. **Zhao, X., and K. Drlica.** 2001. Restricting the selection of antibiotic-resistant mutants: a general strategy derived from fluoroquinolone studies. Clin. Infect. Dis. **33**(Suppl. 3)**:**S147–S156.